ISSN 0915-633X

NATIONAL INSTITUTE FOR FUSION SCIENCE

Model of Divertor Biasing
and
Control of Scrape-off Layer and Divertor Plasmas

K. Nagasaki, K. Itoh and S.-I. Itoh

(Received – Feb. 4, 1991)

NIFS-79 Feb. 1991

RESEARCH REPORT
NIFS Series

NAGOYA, JAPAN

Model of Divertor Biasing and Control of Scrape-off Layer and Divertor Plasmas

Nagasaki, K., Itoh, K.* and Itoh, S.-I.*

Plasma Physics Laboratory, Kyoto University, Uji, Kyoto 611, Japan

**National Institute for Fusion Science, Nagoya 464-01, Japan*

Abstract

Analytic model of the divertor biasing is described. For the given plasma and energy sources from the core plasma, the heat and particle flux densities on the divertor plate as well as scrape-off-layer (SOL)/divertor plasmas are analyzed in a slab model. Using a two-dimensional model, the effects of the divertor biasing and SOL current are studied. The conditions to balance the plasma temperature or sheath potential on different divertor plates are obtained. Effect of the SOL current on the heat channnel width is also discussed.

KEYWORDS: Divertor Biasing, Scrape-off-Layer, Divertor Plasma

§1 Introduction

Recently the importance of scrape-off-layer (SOL) and divertor plasmas has been widely recognized from many view points [1] [2]. The plasmas which surround the main plasma were found to have a critical role in determining the core confinement, particularly for the appearance of the improved confinement modes. The long and stable discharge in the high power heating regime has been possible only if the SOL and divertor plasmas are controlled so that the rapid impurity generation is suppressed. It has also been noticed that the condition which is imposed on the divertor plasma often limits the parameter regime of the consistent fulfillment of various physics and technological constraints[3]. Motivated by these results, investigations have been done in search of the control of SOL/divertor plasmas by the divertor biasing. It has been found that there is a spontaneous force free current in the SOL/divertor region driven by the thermoelectric field [4]. Applying a DC voltage between two divertor plates, efforts were made to control SOL/divertor plasmas [5][6]. Theory was made on the effect of the divertor biasing employing one-dimensional model [7][8]. Response of the plasma parameter to the applied field (or driven current) was studied. Although these works have shown evaluations on the effects, either the energy equation was not appropriate in [7] (as is pointed out in Ref.[9]) and the temperature on divertor plates was not absolutely determined, or only the linear response to the applied voltage was calculated [8]. Further analysis is required to show, at least semi-quantitatively, the effect of the divertor biasing including the two-dimentional nature of SOL/divertor plasmas.

In this article, we extend the analysis in Ref.[7] on the effects of divertor biasing, by employing a simple slab model of the divertor plasma. Assuming the particle flux enhancement factor in the divertor plasma, we evaluate the SOL/divertor plasma parameters as a function of the externally applied DC electric field, for the given fluxes from the core plasma. We

estimate the radial extent of the plasma by assuming a temperature and density dependence of the thermal conductivity. The effect of the DC field on the SOL width is also estimated. We calculate the necessary voltage in order to equalize the plasma temperature or sheath potential at the divertor regions. These parameters are key factors in order to estimate the erosion rate of or the impurity source from the divertor plate[2]. For instance, the control of the sheath potential is effective in reducing the impurity source/erosion rate, because the sputtering yield ratio is a strong nonlinear function of the sheath potential.

In Sec.2, we describe model and equations used in this paper. The linear response of SOL/divertor plasmas is described in Sec.3 and numerical results are shown in Sec.4. Summary and discussion are found in Sec.5.

§2 Model and Equations

The plasma region of our interest is illustrated schematically in Fig.1. We take a simple slab plasma model for the analysis by choosing the radial width of the plasma to be constant along the field line. This simplification allows an analytic treatment. Figure 2 shows a simplified geometry of our analysis. The power and particle flux are supplied from the main plasma at a distance of L_1 from the divertor plate 1. The asymmetry of the source distance between in- and outer divertor plates appears in the experiments. It is usually considered that the heat and particle supplies to the SOL region are given in the vicinity of the outer mid plane.

We assume that there is an external DC power supply and the force free current flows by the thermoelectric field and external field. The equations governing the plasma are as follows [1][10]

• Particle flux density at the divertor plate

$$\Gamma_j = A\, n_j\, T_j^{1/2} \tag{1}$$

• Heat flux density at the divertor plate

$$q_j = \Gamma_j\, T_j\{2 + \phi_j + 2\alpha \exp(-\phi_j)\} \tag{2}$$

• Current density

$$J_j = e\, \Gamma_j\{1 - \exp(\phi - \phi_j)\} \tag{3}$$

where the suffix j (=1, 2) stands for each divertor plate. Notations are n: plasma density, T: temperature (where $T_e = T_i$ is assumed), ϕ_j: ratio of the sheath potential Φ_j to the divertor temperature, $\phi_j = e\Phi_j/T_j$, $\alpha = \sqrt{m_i/4\pi m_e}$, $A = \sqrt{2/m_i}$ and $\phi = \ln[(1-\gamma)\alpha]$. γ is the secondary electron emission coefficient, which is assumed to be $\gamma = 0$. At $\phi_j = \phi$, the heat transmission coefficient $q/\Gamma T = 2 + \phi_j + 2\alpha \exp(-\phi_j)$ is about 6.5 and no SOL current is driven.

The energy balance equation gives the relation

$$T_0^{7/2} = T_j^{7/2} + \frac{7}{2\kappa_0}\, L_j\, q_j \tag{4}$$

where the suffix 0 indicates the value at the source location, and the classical thermal conductivity is assumed as $\kappa_{\|} = \kappa_0\, T^{2.5}$. The heat flux density q_0 and the total power supply to the SOL, P_0, have a relation

$$q_0 = \frac{P_0}{2\pi R\Delta}\, \frac{B_p}{B_t} \tag{5}$$

where Δ is the SOL width, which is determined later. R is the major radius of the torus, B_p and B_t are poloidal and toroidal magnetic fields, respectively. The pressure balance equation yields

$$n_j\, T_j = \frac{1}{2}\, n_0\, T_0. \tag{6}$$

The current is assumed to be divergence free and we have

$$J = J_1 = -J_2. \tag{7}$$

By integrating the Ohm's law along the field line and using Eq.(4), we have

$$V_{ext} = C\ \eta_{\|}(0) L\ J + \Phi_1 - \Phi_2 + \frac{1}{e}(\gamma_p - \gamma_t)(T_1 - T_2) \tag{8}$$

where the constant C is given as $C_1 + C_2$ and

$$C_j = \frac{7}{4}\ \frac{T_0^{3/2}(T_0^2 - T_j^2)}{T_0^{7/2} - T_j^{7/2}}\ \frac{L_j}{L}, \tag{9}$$

γ_p, γ_t are coefficients of the presheath and thermoelectric effects, respectively. For hydrogen plasma, we may choose $\gamma_p = 0.5$ [2] and $\gamma_t = 0.7$ [11]. Voltage drop due to the external resistance is included in the applied voltage V_{ext}. (The relation (8) is obtained by noting the parallel conductivity $\eta_{\|} = \eta_0\ T^{-3/2}$. In the case that q_j can be assumed to be constant along the field line, T_j is expressed as

$$T_j = \left[T_0^{7/2} - \frac{7}{2\kappa_0}\ \ell\ q_j\right]^{2/7} \tag{10}$$

from Eq.(4). Substituting Eq.(10) to the voltage drop of $\int J\eta d\ell$, Eq.(8) is obtained [12].)

The distance between two divertor plates is fixed as

$$L_1 + L_2 = 2L. \tag{11}$$

If we neglect the energy loss in the SOL region, the energy conservation relation can be written as

$$q_1 + q_2 = q_0. \tag{12}$$

The density conservation relation can be written as

$$\frac{\Gamma_1}{G_1} + \frac{\Gamma_2}{G_2} = \Gamma_0 \tag{13}$$

where G is the enhancement factor of the particle flux by the localized recycling near divertor plate.

The expression of Δ is obtained by solving the radial diffusion equation with the parallel loss term. In the absence of the electric field, we have [13]

$$\Delta = 2\pi^2 \; a \; R \; \kappa_B \; T_0^2 \; P^{-1} \tag{14}$$

where a is the minor radius. We here simply assume that the perpendicular thermal conductivity is Bohm-like as

$$\kappa_\perp = \kappa_B \; T. \tag{15}$$

The coefficient κ_B is given as $\kappa_B = \beta \; n_0/16B$, where β is an enhancement factor. Equations (4)(5) and (14) determines the heat channel width self-consistently. In the limit $T_0^{7/2} \gg T_j^{7/2}$, the heat channel width is given as

$$\Delta = \left(2\pi^2\right)^{7/11} \left(\frac{7}{4\pi}\right)^{4/11} (a \; R)^{7/11} \left(\frac{L}{R}\frac{B_p}{B_t}\right)^{4/11} P^{-3/11} \; \kappa_B^{7/11} \; \kappa_0^{-4/11}. \tag{16}$$

If the electric field exists, the $E \times B$ flow is driven by the poloidal electric field. Estimating the poloidal electric field by Φ/a, we have

$$q_r = -\kappa_\perp \frac{\partial T}{\partial r} + \frac{n_0 \; T_0}{B} \frac{\Phi}{a} \tag{17}$$

instead of $q_r = -\kappa_\perp \; \partial T/\partial r$. Evaluating $\partial T/\partial r$ by $-T/\Delta$, we have $q_r = -\kappa'_\perp \; \partial T/\partial r$ with

$$\kappa'_\perp = \; \kappa'_B T \tag{18}$$

and

$$\kappa'_B = \left[1 + \frac{16}{\beta}\frac{e\Phi}{T_0}\frac{\Delta}{a}\right] \kappa_B. \tag{19}$$

In case that the SOL current is in the counter-direction to the core plasma current, the pinch of the heat channel occurs (Φ_1 and Φ_2 work in the same direction). In case that the SOL

current is in the co-direction, the heat channel increases. As a result, we write

$$\kappa_B' = \left[1 + \delta \frac{16}{\beta} \left|\frac{e\Phi}{T_0}\right| \frac{\Delta}{a}\right] \kappa_B \tag{20}$$

and take $\delta = 1$ in the case of co-current in the SOL and $\delta = -1$ in the case of counter-current in the SOL. Replacing κ_B by κ_B' in Eq.(16), we have

$$\Delta = \left[1 + \delta \frac{16}{\beta} \left|\frac{e\Phi}{T_0}\right| \frac{\Delta}{a}\right]^{7/11} \Delta_* \tag{21}$$

where the suffix $*$ indicates the value in the absence of the radial electric field.

We finally note the model of the enhancement factor G. Main part of our analysis is made by assuming G to be constant. This assumption may be valid for the small flux limit or the dense and cold divertor plasma. The transition regime is not treated by this simplification. Other choice of the assumption is that n_j is to be fixed. This case is described in Appendix.

§3 Linear Response

Before showing numerical results, we will analyze the linear response of the SOL/ divertor plasmas. If the source position of the particle and heat flux is a little shifted from the mid point, the SOL length is written as

$$L_j = \overline{L} \mp \tilde{L} \tag{22}$$

where $|\tilde{L}/\overline{L}| \ll 1$. In this case, the SOL width is assumed to the constant, since $|16e\Phi/\beta T_0| \ll 1$ and $\Delta/a \ll 1$. Under this assumption, the plasma parameters can be obtained by linearizing

Eqs.(1)-(8) in the following form

$$\begin{aligned} \Gamma_j &= \overline{\Gamma} \pm \tilde{\Gamma} \\ q_j &= \overline{q} \pm \tilde{q} \\ n_j &= \overline{n} \pm \tilde{n} \\ T_j &= \overline{T} \pm \tilde{T} \\ \phi_j &= \overline{\phi} \pm \tilde{\phi} \end{aligned} \tag{23}$$

where

$$\begin{aligned} \overline{\Gamma} &= \frac{G\Gamma_0}{2} \\ \overline{q} &= \frac{q_0}{2} \\ \overline{n} &= \frac{f(\overline{\phi})^{1/2}\,(G\Gamma_0)^{3/2}}{2\,A\,q_0^{1/2}} \\ \overline{T} &= \frac{q_0}{f(\overline{\phi})\,G\,\Gamma_0} \\ \overline{\phi} &= \ln[(1-\gamma)\alpha] \\ f(\overline{\phi}) &= 2+\overline{\phi}+2\alpha\exp(-\overline{\phi}). \end{aligned} \tag{24}$$

The perturbed quantities are written as

$$\begin{aligned} \tilde{\Gamma} &= \frac{1}{2}\left(-\frac{D_{11}}{D}\,\frac{\tilde{L}}{\overline{L}}+\frac{D_{21}}{D}\,\frac{eV_{ext}}{\overline{\phi}\,\overline{T}}\right)\overline{\Gamma} \\ \tilde{q} &= \left\{\left(1-\frac{D_{11}}{D}\frac{\kappa_0\,\overline{T}^{7/2}}{\overline{q}\,\overline{L}}\right)\frac{\tilde{L}}{\overline{L}}+\frac{D_{21}}{D}\,\frac{\kappa_0\,\overline{T}^{7/2}}{\overline{q}\,\overline{L}}\,\frac{eV_{ext}}{\overline{\phi}\,\overline{T}}\right\}\overline{q} \\ \tilde{n} &= \left(-\frac{D_{11}}{D}\,\frac{\tilde{L}}{\overline{L}}+\frac{D_{21}}{D}\,\frac{eV_{ext}}{\overline{\phi}\,\overline{T}}\right)\overline{n} \\ \tilde{T} &= \left(\frac{D_{11}}{D}\,\frac{\tilde{L}}{\overline{L}}-\frac{D_{21}}{D}\,\frac{eV_{ext}}{\overline{\phi}\,\overline{T}}\right)\overline{T} \\ \tilde{\phi} &= \left(-\frac{D_{12}}{D}\,\frac{\tilde{L}}{\overline{L}}+\frac{D_{22}}{D}\,\frac{eV_{ext}}{\overline{\phi}\,\overline{T}}\right)\overline{\phi} \end{aligned} \tag{25}$$

where

$$
\begin{aligned}
D_{11} &= 2+\frac{e\overline{\Gamma}C\eta_{\parallel}(0)\overline{L}}{\overline{T}} \\
D_{12} &= 2\frac{\overline{\phi}+\gamma_p-\gamma_t}{\overline{\phi}} \\
D_{21} &= \frac{\overline{\phi}\{1-2\alpha\exp(-\overline{\phi})\}}{f(\overline{\phi})} \\
D_{22} &= \frac{(2\kappa_0\overline{T}^{5/2}+f(\overline{\phi})\,\overline{\Gamma L})\,\overline{T}}{2\,\overline{q}\,\overline{L}} \\
D &= D_{11}D_{22}-D_{12}D_{21}.
\end{aligned}
\tag{26}
$$

The parallel current flow is given by

$$
J = e\,\overline{\Gamma}\,\overline{\phi}\left(-\frac{D_{12}}{D}\frac{\tilde{L}}{\overline{L}}+\frac{D_{22}}{D}\frac{eV_{ext}}{\overline{\phi}\,\overline{T}}\right). \tag{27}
$$

When the divertor plates are floating, e.g., the external circuit does not connect two divertor plates and $J=0$, the perturbed quantities are

$$
\begin{aligned}
\tilde{\Gamma} &= -\frac{1}{2}\,\overline{\Gamma}\,\frac{\tilde{L}}{\overline{L}} \\
\tilde{q} &= \left(1-\frac{\kappa_0\,\overline{T}^{7/2}}{\overline{q}\overline{L}}\right)\frac{\tilde{L}}{\overline{q}\overline{L}} \\
\tilde{n} &= -\overline{n}\frac{\tilde{L}}{\overline{L}} \\
\tilde{T} &= \overline{T}\frac{\tilde{L}}{\overline{L}} \\
\tilde{\phi} &= 0.
\end{aligned}
\tag{28}
$$

This indicates that the temperature and heat flux of the divertor plate close to the sources are higher, whereas the density and particle flux are lower.

When two divertor plates are connected by the external circuit, various control is possible. If we want to equalize the temperature of the divertor plates, i.e., $\tilde{T}=0$, we must apply the biased voltage as

$$
V_{ext} = \frac{D_{11}}{D_{21}}\frac{\overline{\phi}\,\overline{T}}{e}\frac{\tilde{L}}{\overline{L}}. \tag{29}
$$

The external power to the SOL plasma is necessary, since the parallel current is not zero from Eq.(27).

The SOL plasma temperature T_0 and density n_0 is hardly charged, since these perturbed terms are 2nd order magnitude of $\tilde{L}/L$. Therfore n_0 and T_0 may be considered to be constant in the linear response as follows,

$$\begin{aligned} n_0 &= 2nT\left(\overline{T}^{7/2} + \frac{7}{2\kappa_0}\,\overline{q}\,\overline{L}\right)^{-2/7} \\ T_0 &= \left(\overline{T}^{7/2} + \frac{7}{2\kappa_0}\,\overline{q}\,\overline{L}\right)^{2/7}. \end{aligned} \tag{30}$$

When $\tilde{L}/\overline{L}$ is not small, we cannot treat the equations linearly. In the next section, we will show numerical results.

§4 Numerical Results

We normalize the model equations for numerical calculations. Normalized parameters are

$$\begin{aligned} &\hat{q} = q/q_* \quad , \quad \hat{\Gamma} = \Gamma/\Gamma_*, \\ &\hat{T} = T/T_* \quad , \quad \hat{n} = n/n_*, \\ &\hat{\Phi} = \Phi/\Phi_* \quad , \quad \hat{V}_{ext} = V_{ext}/V_*, \\ &\hat{J} = J/J_* \quad , \quad \hat{L}_j = L_j/L. \end{aligned} \tag{31}$$

In this section, we take $q_* = 1$ [MW/m^2], $\Gamma_* = 10^{23}$ [1/m^{2}s], $T_* = 1$ [eV], $n_* = 10^{19}$ [1/m^3], $\Phi_* = V_* = 1$ [V], $L = 30$[m] and $J_* = e\Gamma_*$.

We first examine the effect of bias voltage on the heat channel width. Change of the SOL width by the applied voltage is shown in Fig.3. The flux sources from the core plasma and the SOL width in the absence of the applied voltage are chosen as $\hat{q}_0 = 10$, $\hat{\Gamma}_0 = 2$ and $\Delta_*/a = 0.02$. Other fixed parameters are $\hat{L}_1 = 0.75$, $G = 10$ and $\beta = 2$. The solid line is in the case that the SOL current is driven in the direction of the core plasma current($\delta = 1$), and the dotted line is in the case of counter-direction($\delta = -1$). The SOL width has a nearly linear dependence on the applied voltage and varies with the direction of the $E \times B$ flow.

The variation of SOL/divertor plasma parameters due to the applied voltage are shown in Fig.4 for the same condition as in Fig.3. In this case, we take $\delta = -1$, e.g. the $E \times B$ force makes the inward flow. The case of $\delta = 1$ shows a similar behavior. This is because the change of the SOL width does not exceed 20 % for the range of present analysis, and remains to be a small correction. When no external bias is applied, T_1 is higher than T_2, since the flux source is chosen close to the divertor plate 1. The divertor temperature can be equalized at $\hat{V}_{ext} \simeq 100$. The sheath potential can be also equalized at $\hat{V}_{ext} \simeq -54$. These results imply that the divertor temperature or sheath potential can be balanced by the DC divertor biasing. The SOL plasma parameters n_0 and T_0 are weakly changed. Control of the boundary condition of the core plasma by this divertor biasing method may be difficult. We should also note the change of the heat and particle flux densities. The particle flux densities toward two divertor plates are equalized at $T_1 = T_2$, while the heat fluxes are not, since the heat transmission coefficients $2 + \phi_j + 2\alpha \exp(-\phi_j)$ have different values between two divertor plates. Numerical calculation confirms the results that the DC biasing hardly changes the heat flux distribution between two divertor plates.

At a large bias voltage, plasma parameters show strong dependence on V_{ext}. For the divertor plate 1, $d\hat{\Phi}_1/d\hat{V}_{ext}$ is positive at $\hat{V}_{ext} \lesssim 90$ but becomes negative at $\hat{V}_{ext} \gtrsim 90$. Associated with this, T_1 and n_1 change strongly. At a large bias voltage, the SOL current toward the plate 1 is carried by the ion saturation current. Since the factor $1 - \exp(\phi - \phi_1)$ in Eq.(3) approaches 1, Γ_1 and J_1 are proportional to $T_j^{-1/2}$ for the fixed value of $n_1 T_1 = n_0 T_0/2$. (Note that $n_0 T_0$ is only slightly changed.) In this ion saturation current regime, the increment of J_1 requires the reduction of T_1, causing the increase of n_1. Similar phenomena can be seen at the plate 2 for the region of $\hat{V}_{ext} \lesssim -100$. The temperature T_2 strongly drops and the density n_2 inceases. In such a large voltage region, the potential drop due to the parallel electric field in

the SOL region is dominant compared to the sheath potential drops.

The SOL current does not become zero when no bias is applied, since the difference between the distributed heat flux densities toward the divertor plates induces the parallel SOL current. This correspond to the thermoelectric current obtained in ref.[4]. There exists the region of applied voltage near $V_{ext} = 0$ in which the plasma works to the external circuit ($V_{ext}J < 0$).

The relation between the total heat flux and external applied voltage necessary for $T_1 = T_2$ or $\Phi_1 = \Phi_2$ is shown in Fig.5. In this case, we take $\delta = -1$. The voltage to balance the divertor temperature has a minimum for a given heat flux. Since the SOL width becomes wider with the decrease of the total heat flux, the substantial heat flux is more smaller, so that the larger voltage is necessary compared to the case of neglecting the $E \times B$ flow. Note that correction is less than order of 10 % as seen in Fig.3. If we take $\delta = 1$, the reverse tendency is obtained. As for the sheath potential, the applied voltage becomes smaller with the increase of heat flux.

Plasma parameters are also functions of the location of the source fluxes from the core plasma. Figure 6 shows the plasma parameters at the voltage to equalize the divertor temperature as a function of source location, L_1/L. It is noted that we have three solutions around $\hat{L}_1 = 1$. One is unstable, which we have obtained analytically in Sec.2, and others are stable, which are characterized by large applied voltage and sheath potential. We can explain this phenomenon using Fig.4(a). When the source location approaches the mid point, the temperature of the plate 1 goes down and that of the plate 2 goes up, so that the solutions appear at the negative voltage. These solutions can be obtained only if the flux source exists close to the mid point. On the other hand, the SOL plasma parameters n_0 and T_0 are hardly changed, which agree with the anlytical estimate. The SOL current and applied voltage only slightly increase even when the input position rather approaches the divertor plate. We also

obtain the numerical results that the distribution of heat and particle flux toward the divertor plates has a linear ralation to the input position.

§4 Summary and Discussion

Control possibility of SOL/divertor plasmas by the external DC biasing was studied. Two-dimensional model was used including the effect of the cross field $E \times B$ flow driven by the SOL current parallel to the magnetic field line. It is found that some of divertor plasma properties can be controlled by the DC divertor biasing. The imbalance of the plasma temperature or sheath potential between the in- and outer divertor plates, which occurs due to the asymmetry of the location of the flux supplies to the SOL region, can be controlled. On the other hand, the influence on the SOL width and SOL plasma parameters n_0 and T_0 remains to be corrections of the order of 10 %. Least sensitive is the heat deposition onto the divertor plates.

The poloidal electric field is formed by the SOL current. We assume the simple Ohms law for the SOL current and the parallel electric field. The question arises whether or not this electric field exceeds the Dreicer limit, which is the critical value of generating runaway electrons. The Dreicer limit is given by [14]

$$E_{cr} = \frac{e \ln \Lambda}{8\pi\epsilon_0 \lambda_D} \tag{32}$$

where Λ and λ_D is the Coulomb logarithm and Debye length, respectively. The critical SOL current to reach the Dreicer limit can be given as

$$J_{cr} = 2.4 \times 10^{-13} n T^{1/2}. \tag{33}$$

For example, provided that $n = 10^{19}[m^{-3}]$ and $T = 10[eV]$, we have $J_{cr}/J_* \simeq 4.7 \times 10^2$, which is large 2 order magnitude compared to the SOL current calculated in present analysis. Therefore we may use the Ohm's law for the evaluation of the SOL current.

At the voltage, $\hat{V}_{ext} = 100$, which is necessary for $T_1 = T_2$ in Fig.4, the external power given to the core plasma is about 16 [MW/m^2]. This is the same order as the outward power flow from the core plasma. In case of equalizing the sheath potential ($\hat{V}_{ext} = -54$), the external power is about 6.3 [MW/m^2]. Our model indicates that the external power is necessary to be large in such a case of asymmetry $L_2/L_1 = 5/3$. In order to treat correctly this strong asymmetry, the Joule heating of the SOL plasma by external voltage must be kept in the energy balance equation. This is left for future work.

In this paper, though two dimensional effects are taken into accout by a model, effects of impurities and neutrals are not directly included. Impureties radiate the heat power and the enhancement factor of the particle flux G is a function of neutral densities. More quantitative analysis such as the numerical simulation by UEDA code[15] is required to compare with the experimental results.

We finally note the effect of the divertor biasing on a core confinement. This analysis shows order of 10 % correction to the boundary condition of the core plasma. The analysis is made under the assumption that the source from the core is constant. It is well known, however, that slight change of the boundary condition can cause dramatic change of the core plasma such as the H-mode [16]. In experiments, applied bias voltage may vary across the magnetic surface, causing the radial electric field. More complete anlysis combining with the bifurcation phenomena[17] of the core plasma requires further research.

Acknowledgement

Authors wish to thank JFT-2M Group, Dr. M. Shimada, Dr. T. Takizuka, Dr. H. Zushi and Dr. T. Mizuuchi for useful discussions. This work was partly supported by the Grant-in-Aid for Scientific Research from the Ministry of Education, Science and Culture of Japan.

Appendix

In this Appendix, we consider the model in which n_j is constant, $n_1 = n_2 = n$. Plasma parameters are solved using Eqs.(1)-(4), (7)-(9), (11) (12) and (21). The SOL density n_0 can not be determined.

First, the linear response is investigated. Similarly in Sec.3, when we assume $L_j = \overline{L} \pm \tilde{L}$ ($|\tilde{L}/\overline{L}| \ll 1$), the plasma parameters are written as

$$\begin{aligned} \Gamma_j &= \overline{\Gamma} \pm \tilde{\Gamma} \\ q_j &= \overline{q} \pm \tilde{q} \\ T_j &= \overline{T} \pm \tilde{T} \\ \phi_j &= \overline{\phi} \pm \tilde{\phi} \end{aligned} \tag{A.1}$$

where

$$\begin{aligned} \overline{q} &= \frac{q_0}{2} \\ \overline{\Gamma} &= An\left[\frac{q_0}{2Anf(\overline{\phi})}\right]^{1/3} \\ \overline{T} &= \left[\frac{q_0}{2Anf(\overline{\phi})}\right]^{2/3} \\ \overline{\phi} &= \ln[(1-\gamma)\alpha]. \end{aligned} \tag{A.2}$$

The perturbed quantities are given as

$$\begin{aligned} \tilde{q} &= \left\{\left(1 - \frac{D_{11}}{D}\frac{\kappa_0\overline{T}^{7/2}}{\overline{q}\,\overline{L}}\right)\frac{\tilde{L}}{\overline{L}} + \frac{D_{21}}{D}\frac{\kappa_0\overline{T}^{7/2}}{\overline{q}\,\overline{L}}\frac{eV_{ext}}{\overline{\phi}\,\overline{T}}\right\}\overline{q} \\ \tilde{\Gamma} &= \frac{1}{2}\left(\frac{D_{11}}{D}\frac{\tilde{L}}{\overline{L}} - \frac{D_{21}}{D}\frac{eV_{ext}}{\overline{\phi}\,\overline{T}}\right)\overline{\Gamma} \\ \tilde{T} &= \left(\frac{D_{11}}{D}\frac{\tilde{L}}{\overline{L}} - \frac{D_{21}}{D}\frac{eV_{ext}}{\overline{\phi}\,\overline{T}}\right)\overline{T} \\ \tilde{\phi} &= \left(-\frac{D_{12}}{D}\frac{\tilde{L}}{\overline{L}} + \frac{D_{22}}{D}\frac{eV_{ext}}{\overline{\phi}\,\overline{T}}\right)\overline{\phi} \\ J &= \left(-\frac{D_{12}}{D}\frac{\tilde{L}}{\overline{L}} + \frac{D_{22}}{D}\frac{eV_{ext}}{\overline{\phi}\,\overline{T}}\right)e\overline{\Gamma}\,\overline{\phi} \end{aligned} \tag{A.3}$$

where the definition of $D_{k\ell}$ is the same as that in Sec.3.

When the divertor plates are floating, $\tilde{\phi} = 0$ and $J = 0$, the perturbed terms of heat and particle fluxes are

$$\begin{aligned} \tilde{\Gamma} &= \frac{1}{2}\overline{\Gamma}\frac{\tilde{L}}{\overline{L}} \\ \tilde{q} &= \frac{3\,\overline{q}^2\,\overline{L}}{3\,\overline{q}\,\overline{L} + \kappa_0\overline{T}^{7/2}}\frac{\tilde{L}}{\overline{L}}. \end{aligned} \tag{A.4}$$

The different point from the results in Sec.3 is that the particle flux increases when the input source is close to the divertor plate. (It decreases in the model of Sec.3.) This is because the particle flux is proportional to $T^{1/2}$ as shown in Eq.(1).

The applied voltage to equalize the temperature of two divertor plates is given as

$$V_{ext} = \frac{D_{11}}{D_{21}}\frac{\overline{\phi}\,\overline{T}}{e}\frac{\tilde{L}}{\overline{L}} \tag{A.5}$$

which agrees with the solution (29).

The voltage to equalize the heat flux can be also obtained as follows,

$$V_{ext} = \frac{D_{11}\,\kappa_0\overline{T}^{7/2} - D\overline{q}\,\overline{L}}{D_{21}\,\kappa_0\overline{T}^{7/2}}\frac{\overline{\phi}\,\overline{T}}{e}\frac{\tilde{L}}{\overline{L}}. \tag{A.6}$$

This voltage value is very large, since $\kappa_0\overline{T}^{7/2}/L \ll \overline{q}$.

We numerically investigate the relation between the plasma parameters and applied voltage. The divertor plasma can be also controlled in this model, e.g., the divertor temperature or sheath potential can be balanced. For $n_j = 5\times10^{19}[1/m^3]$, $q_0 = 10[MW/m^2]$ and $L_1/L = 0.75$, the necessary voltage for $T_1 = T_2$ and $\Phi_1 = \Phi_2$ are $V_{ext} \simeq 110$ and $-30[V]$ and the external powers are 14 and 1.5 $[MW/m^2]$. It is surprizing that the SOL current begins to decrease when the applied voltage is beyond a certain value. This can be explained as follows; at a large positive voltage, the SOL current have a strong dependence on T_1, since n_1 is fixed and $1 - \exp(\phi - \phi_1) \to 1$ in Eq.(3). As T_1 decreases, the SOL current is a decreasing function of applied voltage. It is also noted that we have numerical results that n_0 and T_0 weakly changes, which is similar to the model that Γ_0 is fixed.

Figure Caption

Fig.1 Geometry of the plasma region.

Fig.2 Slab model of the SOL/divertor plasmas.

Fig.3 SOL width as a function of applied voltage. Real and dotted lines correspond to the cases for $\delta = 1$ and $\delta = -1$, respectively.

Fig.4 Relation between plasma parameters and applied voltage, (a)temperature, (b)density, (c)sheath potential and (d)SOL current. The condtions are the same as those in Fig.3.

Fig.5 External applied voltage necessary for $T_1 = T_2$ or $\Phi_1 = \Phi_2$. Real and dotted lines correspond to $T_1 = T_2$ and $\Phi_1 = \Phi_2$ cases, respectively. Total particl flux is (a)$\hat{\Gamma}_0 = 1$, (b)$\hat{\Gamma}_0 = 2$ and (c)$\hat{\Gamma}_0 = 5$.

Fig.6 Plasma parameters as a function of input position of the heat and particle fluxes when the temperature at two divertor plates is balanced. (a)temperature, (b)density, (c)sheath potential. Total heat and particle fluxes are chosen as $\hat{q}_0 = 10$ and $\hat{\Gamma}_0 = 2$.

References

[1] Wagner, F. and Lackner, K.: in Physics of Plasma-Wall Interactions in Controlled Fusion (Proc. NATO Advanced Study Institute, 1984) NATO ASI Series, Vol.131, Plenum Press, New York (1986) 931.

[2] Stangeby, P.C.: Nucl. Fusion 30 (1990) 1225.

[3] Itoh, S.-I., Fukuyama, A., Takizuka, T., and Itoh, K.: Fusion Technology 16 (1989) 346.

[4] Harbour, P.J., Summers, D.D.R., Clement, S., *et al.*: J. Nucl. Mat. 162-164 (1989) 236.

[5] Mahdavi, M.A. and D-III D Team: in *Plasma Physics and Controlled Nuclear Fusion Research* (Proc. 13th Int. Conf., Washington, 1990) IAEA-CN-53/I-1-1.

[6] Miura, Y. and JFT-2M Team: in *Plasma Physics and Controlled Nuclear Fusion Research* (Proc. 13th Int. Conf., Washington, 1990) IAEA-CN-53/A-4-6.

[7] Staebler, G.M. and Hinton, F.L.: Nucl. Fusion 29 (1989) 1820.

[8] Itoh, K. (ed.): "Electric Field and Confinement in Toroidal Plasma" (1988,Kyoto) Chap.5 in Japanese.

[9] Stangeby, P.C.: Nucl. Fusion 30 (1990) 1153.

[10] Stangeby, P.C.: in Physics of Plasma-Wall Interactions in Controlled Fusion (Proc. NATO Advanced Study Institute, 1984) NATO ASI Series, Vol.131, Plenum Press, New York (1986) 41.

[11] Hinton, F.L.: in Handbook of Plasma Physics (Rosenbluth, M.N. and Sagdeev, R.Z., eds.) Vol.1, North-Holland, Amsterdam (1983) 147.

[12] Shimada, M.: private communication (1989).

[13] Itoh, K., Nagasaki, K., Itoh, S.-I. and Fukuyama, A: Nucl. Fusion 29 (1989) 1299.

[14] Spitzer, L., JR.: in Physics of Fully Ioized Gases (1962, Interscience, New York)

[15] Ueda, N., Itoh, K. and Itoh, S.-I.: Nucl. Fusion 29 (1989) 1602.

[16] ASDEX Team: Nucl. Fusion 29 (1989) 1959.

[17] Itoh, S.-I. and Itoh, K.: Phys. Rev. Lett. 60 (1988) 2276.

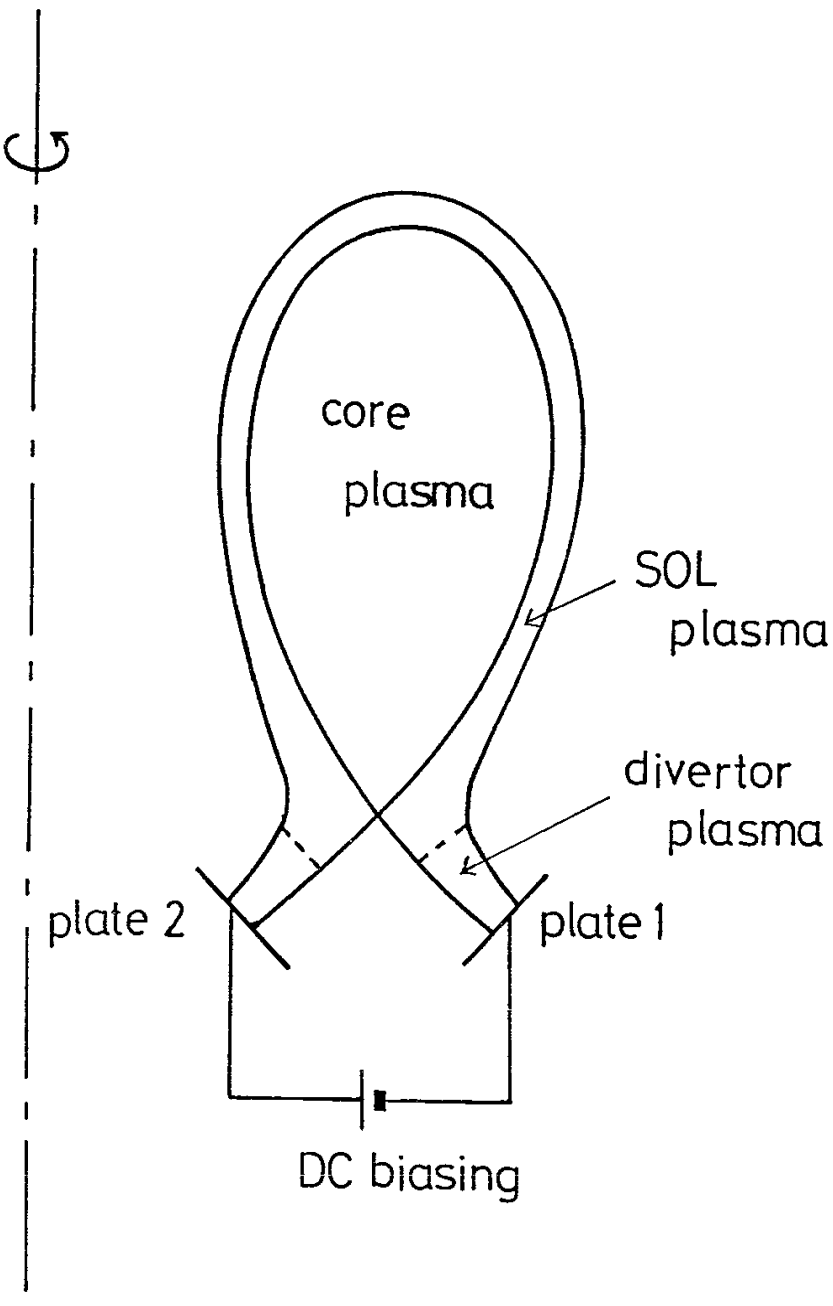
core
plasma
SOL
plasma
divertor
plasma
plate 2
plate 1
DC biasing

Fig.1

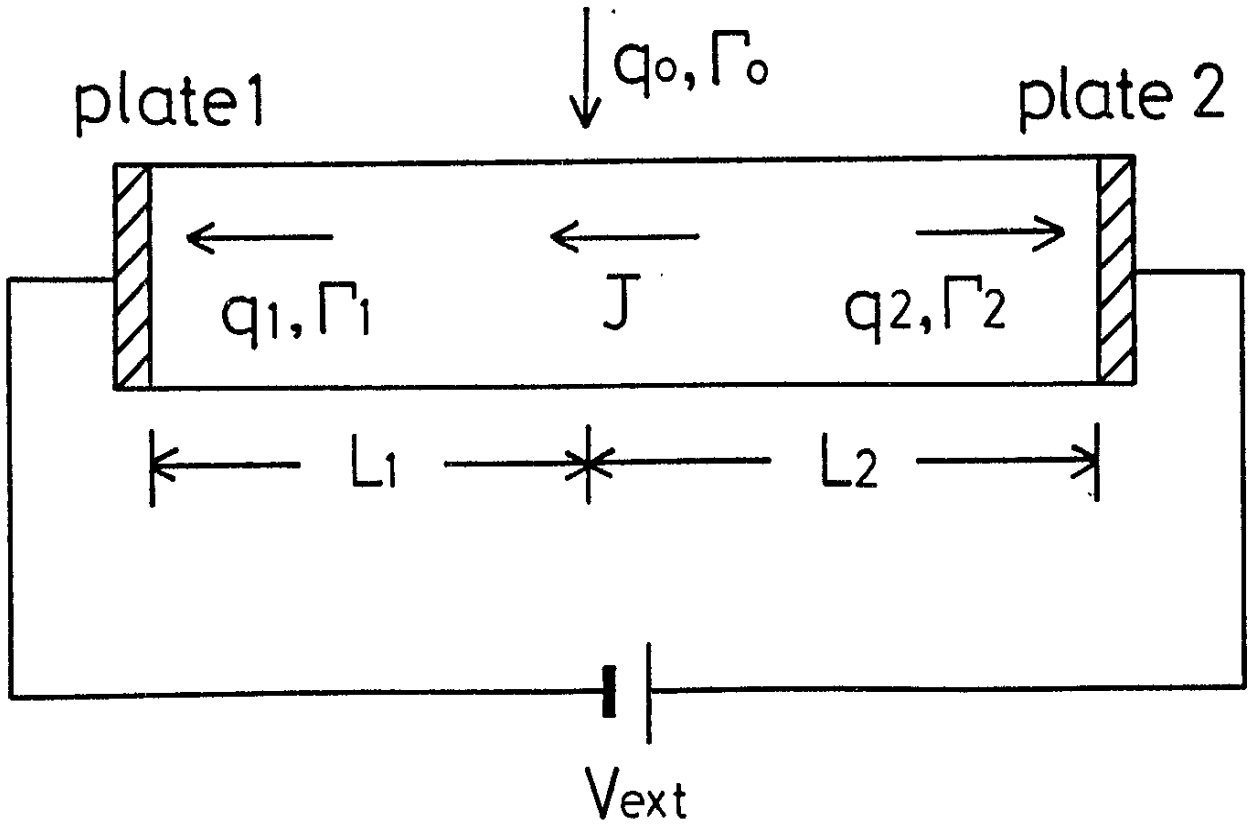

Fig. 2

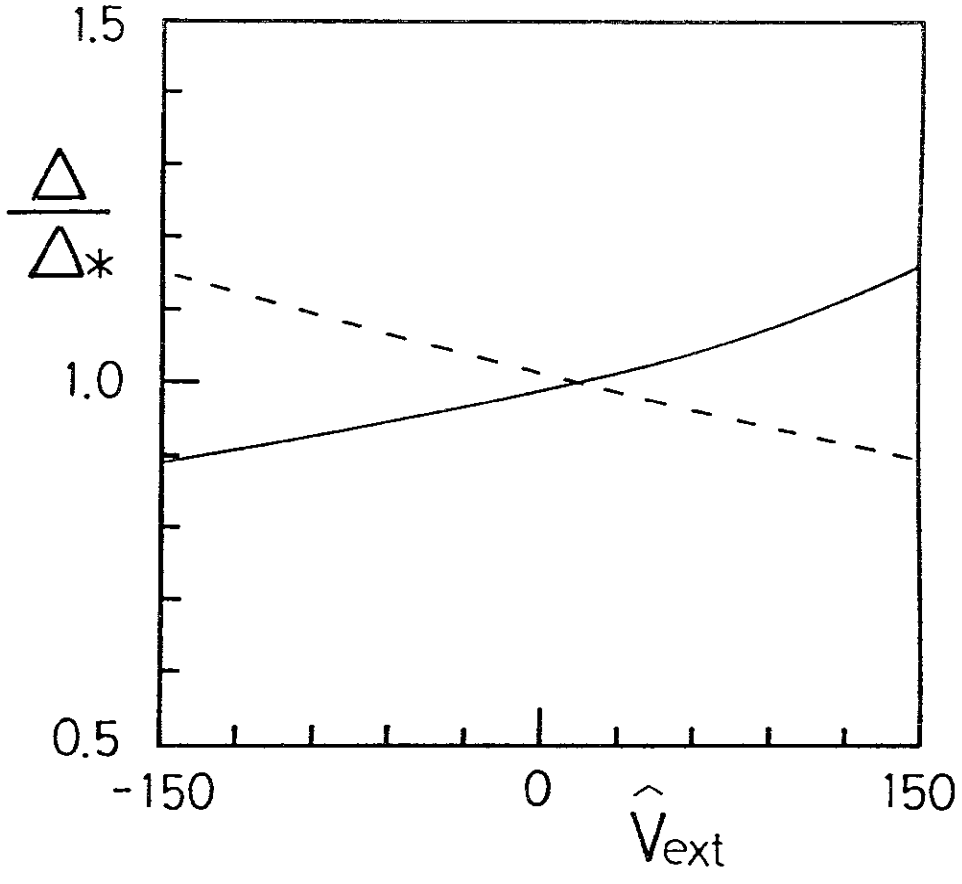

Fig. 3

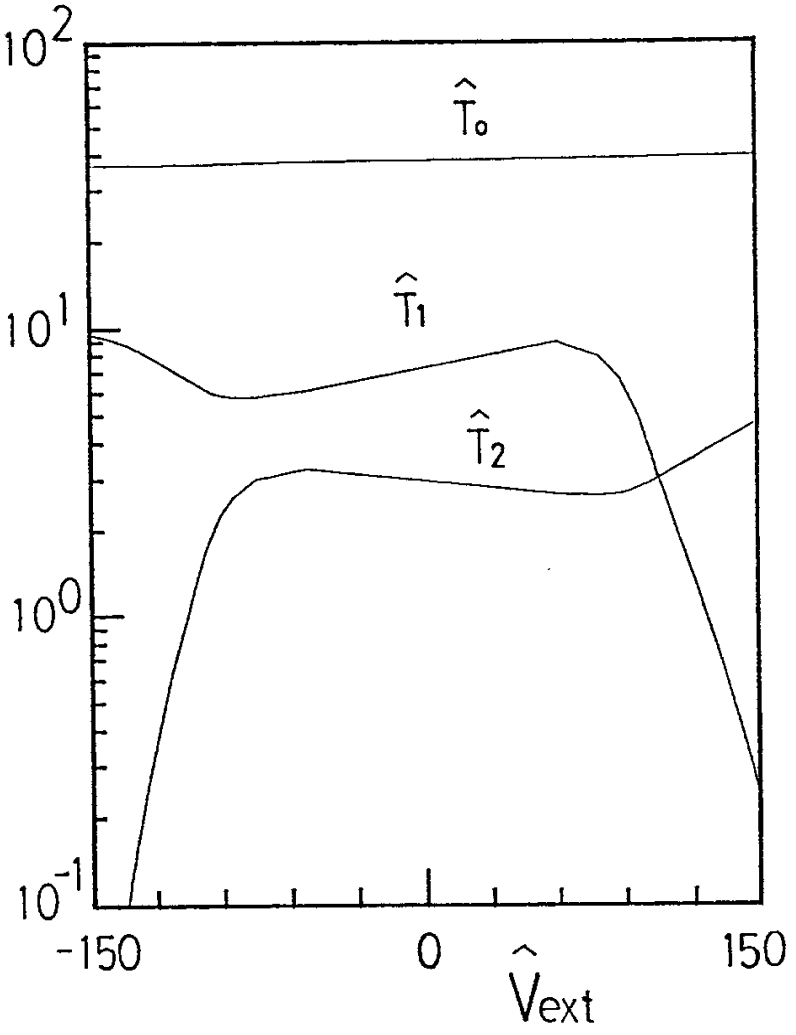

Fig. 4(a)

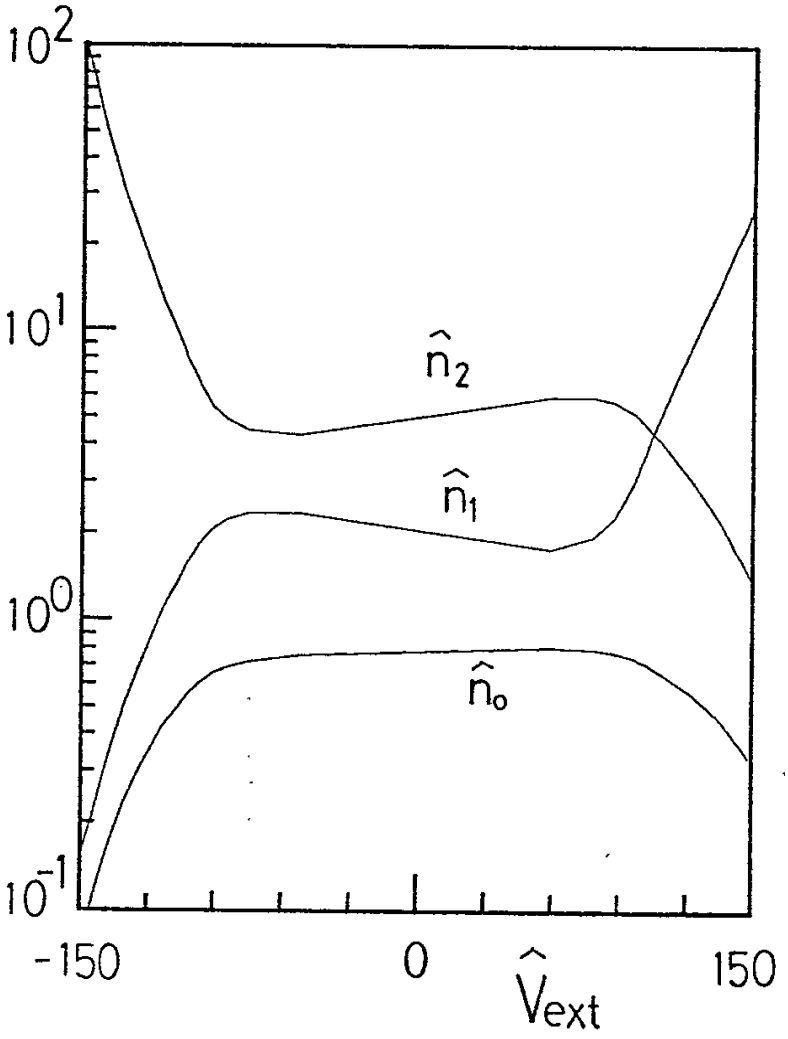

Fig. 4(b)

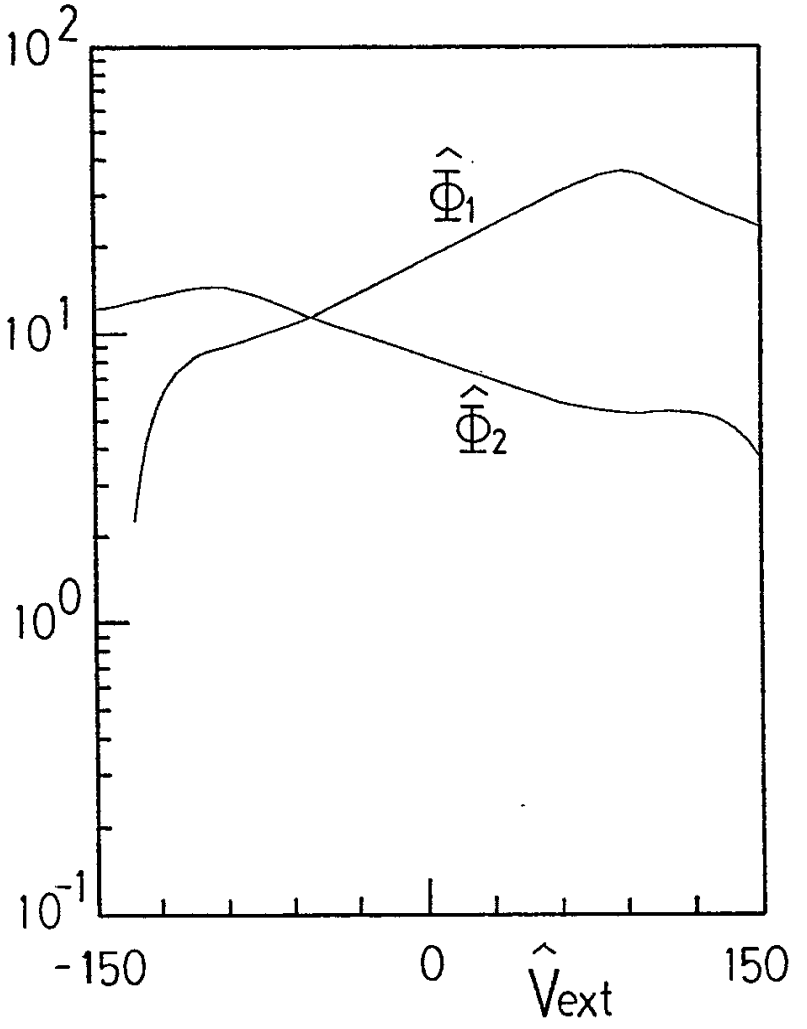

Fig. 4(c)

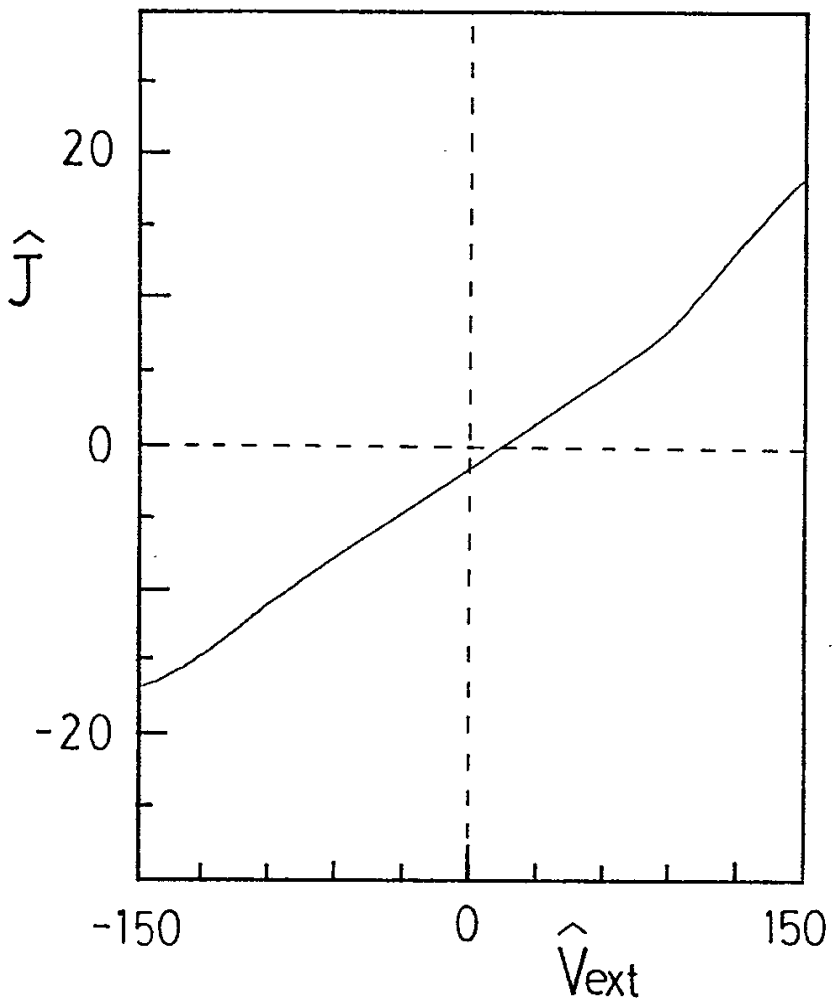

Fig. 4(d)

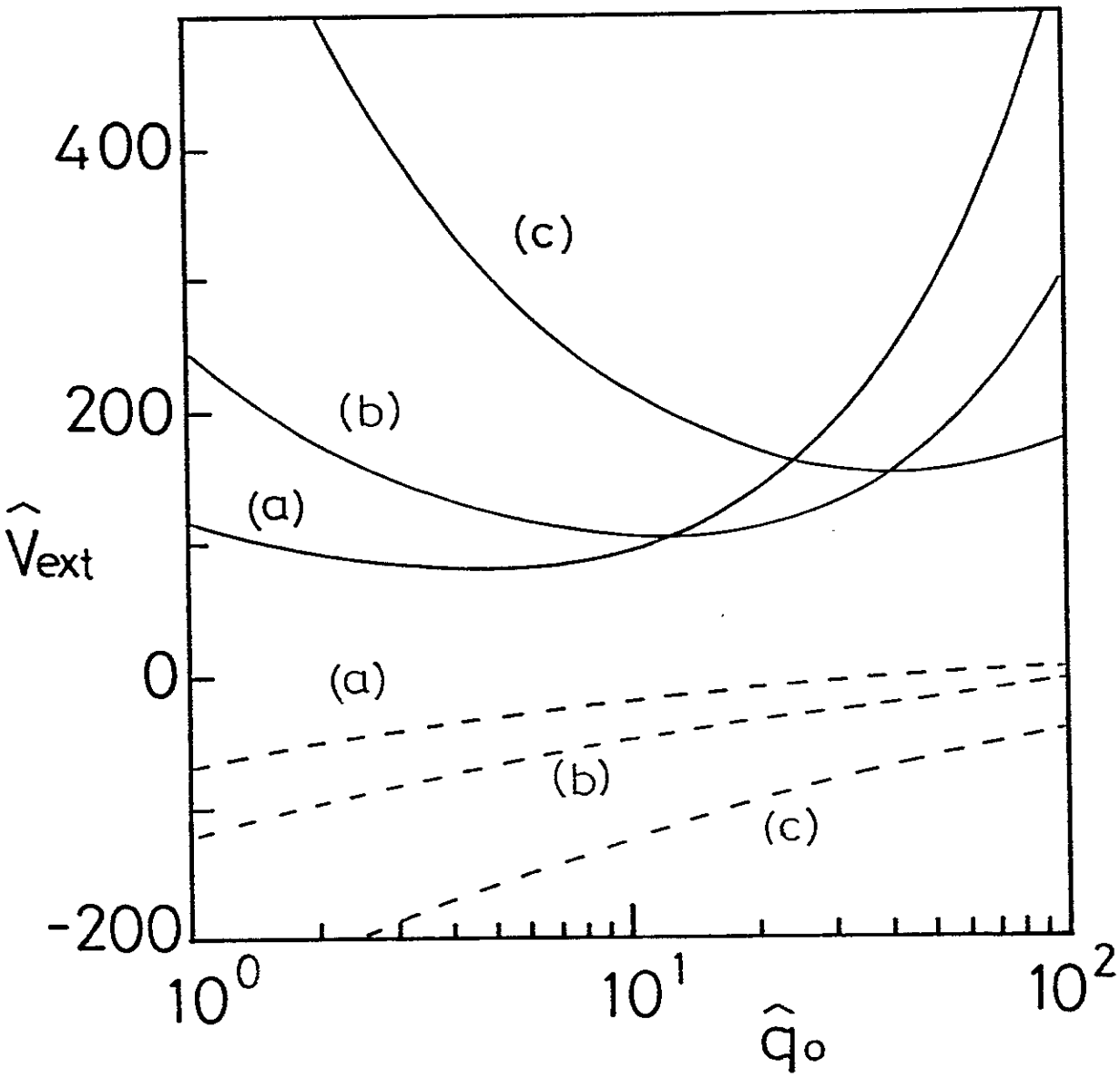

Fig. 5

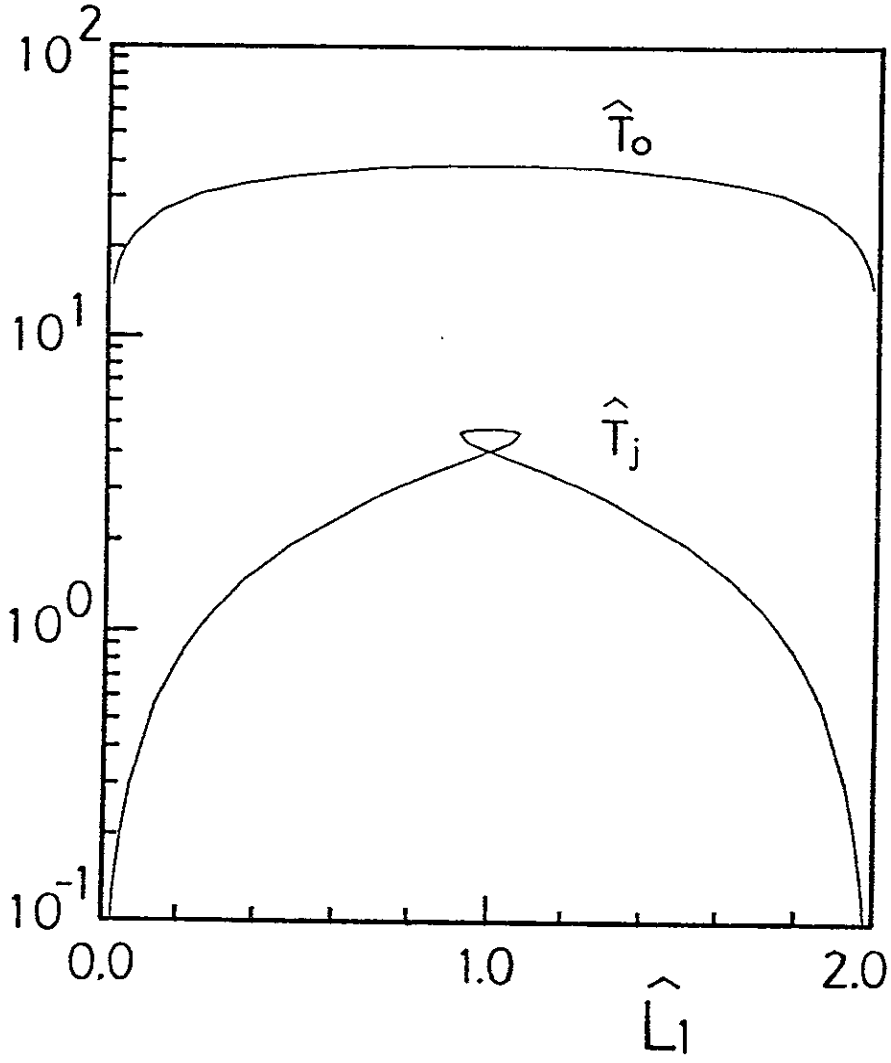

Fig. 6(a)

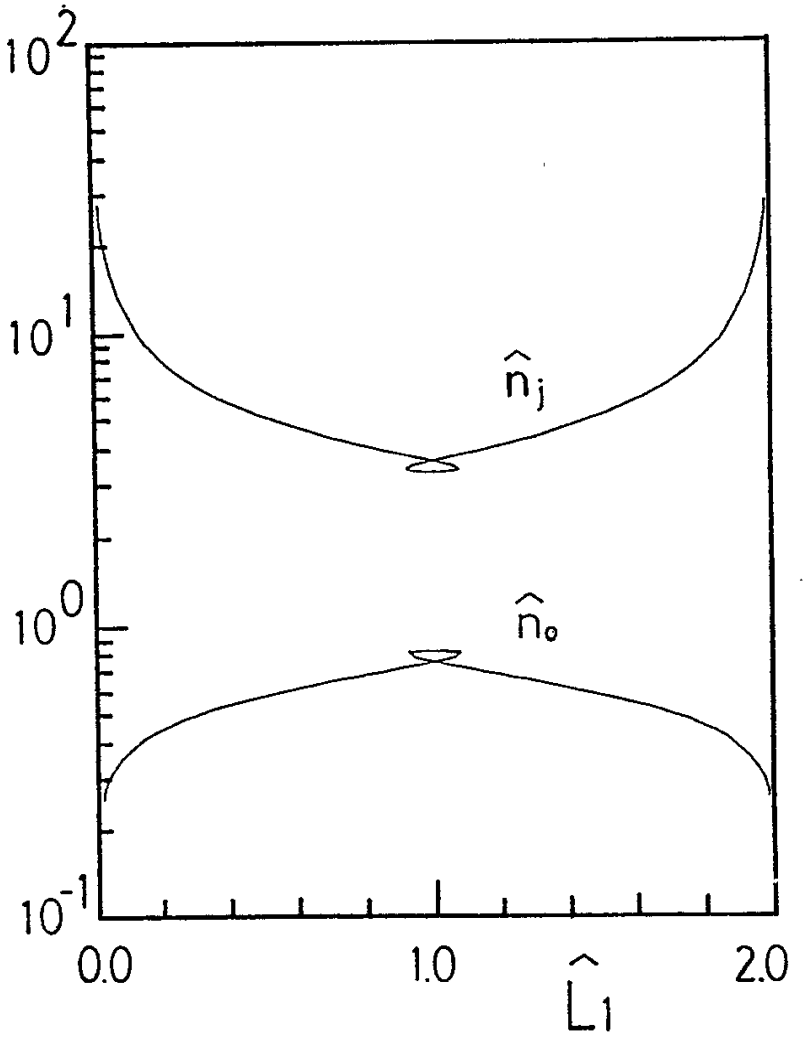

Fig. 6(b)

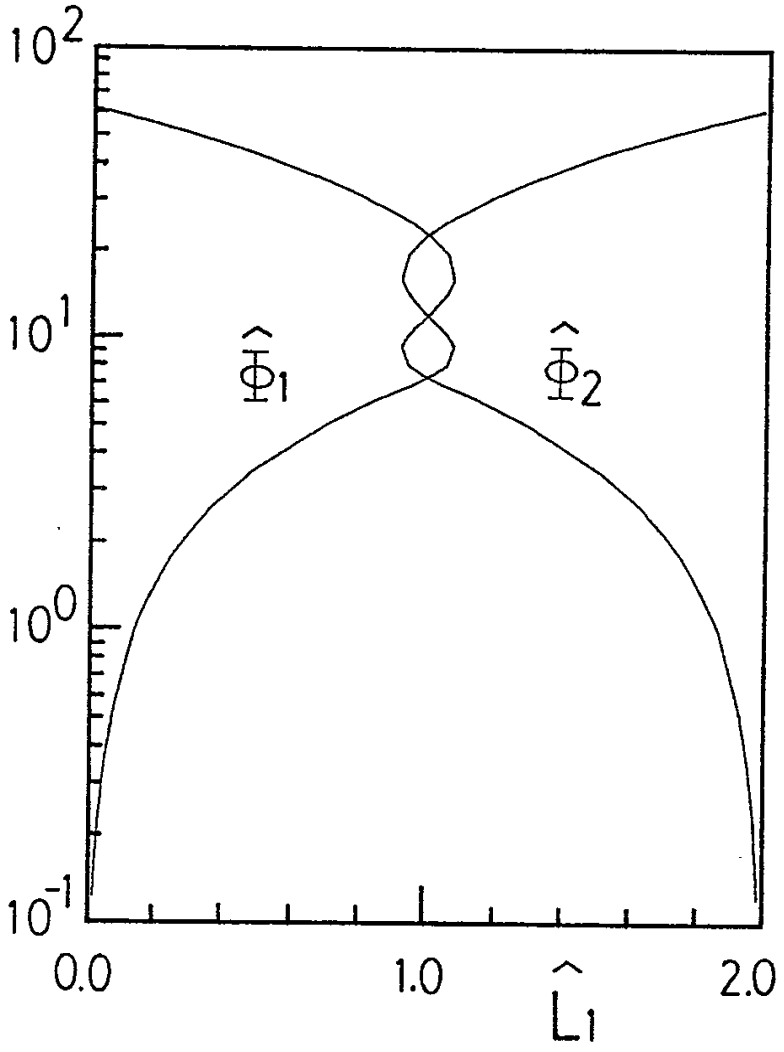

Fig. 6(c)

Recent Issues of NIFS Series

NIFS-30 K. Yamazaki, O. Motojima, M. Asao, M. Fujiwara and A. Iiyoshi, *Design Scalings and Optimizations for Super-Conducting Large Helical Devices* ; May 1990

NIFS-31 H. Sanuki, T. Kamimura, K. Hanatani, K. Itoh and J. Todoroki, *Effects of Electric Field on Particle Drift Orbits in a $l=2$ Torsatron* ; May 1990

NIFS-32 Yoshi H. Ichikawa, *Experiments and Applications of Soliton Physics*; June 1990

NIFS-33 S.-I. Itoh, *Anomalous Viscosity due to Drift Wave Turbulence* ; June 1990

NIFS-34 K. Hamamatsu, A. Fukuyama, S.-I. Itoh, K. Itoh and M. Azumi, *RF Helicity Injection and Current Drive* ; July 1990

NIFS-35 M. Sasao, H. Yamaoka, M. Wada and J. Fujita, *Direct Extraction of a Na- Beam from a Sodium Plasma* ; July 1990

NIFS-36 N. Ueda, S.-I. Itoh, M. Tanaka and K. Itoh, *A Design Method of Divertor in Tokamak Reactors* Aug. 1990

NIFS-37 J. Todoroki, *Theory of Longitudinal Adiabatic Invariant in the Helical Torus*; Aug. 1990

NIFS-38 S.-I. Itoh and K. Itoh, *Modelling of Improved Confinements – Peaked Profile Modes and H-Mode–* ; Sep. 1990

NIFS-39 O. Kaneko, S. Kubo, K. Nishimura, T. Syoji, M. Hosokawa, K. Ida, H. Idei, H. Iguchi, K. Matsuoka, S. Morita, N. Noda, S. Okamura, T. Ozaki, A. Sagara, H. Sanuki, C. Takahashi, Y. Takeiri, Y. Takita, K. Tsuzuki, H. Yamada, T. Amano, A. Ando, M. Fujiwara, K. Hanatani, A. Karita, T. Kohmoto, A. Komori, K. Masai, T. Morisaki, O. Motojima, N. Nakajima, Y. Oka, M. Okamoto, S. Sobhanian and J. Todoroki, *Confinement Characteristics of High Power Heated Plasma in CHS*; Sep. 1990

NIFS-40 K. Toi, Y. Hamada, K. Kawahata, T. Watari, A. Ando, K. Ida, S. Morita, R. Kumazawa, Y. Oka, K. Masai, M. Sakamoto, K. Adati, R. Akiyama, S. Hidekuma, S. Hirokura, O. Kaneko, A. Karita, T. Kawamoto, Y. Kawasumi, M. Kojima, T. Kuroda, K. Narihara, Y. Ogawa, K. Ohkubo, S. Okajima, T. Ozaki, M. Sasao, K. Sato, K.N. Sato, T. Seki, F. Shimpo, H. Takahashi, S. Tanahashi, Y. Taniguchi and T. Tsuzuki, *Study of Limiter H- and IOC- Modes by Control of Edge Magnetic Shear and Gas Puffing in the JIPP T-IIU Tokamak*; Sep. 1990

NIFS-41 K. Ida, K. Itoh, S.-I. Itoh, S. Hidekuma and JIPP T-IIU & CHS Group, *Comparison of Toroidal/Poloidal Rotation in CHS Heliotron/Torsatron and JIPP T-IIU Tokamak*; Sep .1990

NIFS-42 T.Watari, R.Kumazawa,T.Seki, A.Ando,Y.Oka, O.Kaneko, K.Adati, R.Ando, T.Aoki, R.Akiyama, Y.Hamada, S.Hidekuma, S.Hirokura, E.Kako, A.Karita, K.Kawahata, T.Kawamoto, Y.Kawasumi, S.Kitagawa, Y.Kitoh, M.Kojima, T. Kuroda, K.Masai, S.Morita, K.Narihara, Y.Ogawa, K.Ohkubo, S.Okajima, T.Ozaki, M.Sakamoto, M.Sasao, K.Sato, K.N.Sato, F.Shinbo, H.Takahashi, S.Tanahashi, Y.Taniguchi, K.Toi, T.Tsuzuki, Y.Takase, K.Yoshioka, S.Kinoshita, M.Abe, H.Fukumoto, K.Takeuchi, T.Okazaki and M.Ohtuka, *Application of Intermediate Frequency Range Fast Wave to JIPP T-IIU and HT-2 Plasma*; Sep. 1990

NIFS-43 K.Yamazaki, N.Ohyabu, M.Okamoto, T.Amano, J.Todoroki, Y.Ogawa, N.Nakajima, H.Akao, M.Asao, J.Fujita, Y.Hamada, T.Hayashi, T.Kamimura, H.Kaneko, T.Kuroda, S.Morimoto, N.Noda, T.Obiki, H.Sanuki, T.Sato, T.Satow, M.Wakatani, T.Watanabe, J.Yamamoto, O.Motojima, M.Fujiwara, A.Iiyoshi and LHD Design Group, *Physics Studies on Helical Confinement Configurations with l=2 Continuous Coil Systems*; Sep. 1990

NIFS-44 T.Hayashi, A.Takei, N.Ohyabu, T.Sato, M.Wakatani, H.Sugama, M.Yagi, K.Watanabe, B.G.Hong and W.Horton, *Equilibrium Beta Limit and Anomalous Transport Studies of Helical Systems*; Sep. 1990

NIFS-45 R.Horiuchi, T.Sato, and M.Tanaka, *Three-Dimensional Particle Simulation Study on Stabilization of the FRC Tilting Instability*; Sep. 1990

NIFS-46 K.Kusano, T.Tamano and T. Sato, *Simulation Study of Nonlinear Dynamics in Reversed-Field Pinch Configuration*; Sep. 1990

NIFS-47 Yoshi H.Ichikawa, *Solitons and Chaos in Plasma*; Sep. 1990

NIFS-48 T.Seki, R.Kumazawa, Y.Takase, A.Fukuyama, T.Watari, A.Ando, Y.Oka, O.Kaneko, K.Adati, R.Akiyama, R.Ando, T.Aoki, Y.Hamada, S.Hidekuma, S.Hirokura, K.Ida, K.Itoh, S.-I.Itoh, E.Kako, A. Karita, K.Kawahata, T.Kawamoto, Y.Kawasumi, S.Kitagawa, Y.Kitoh, M.Kojima, T.Kuroda, K.Masai, S.Morita, K.Narihara, Y.Ogawa, K.Ohkubo, S.Okajima, T.Ozaki, M.Sakamoto, M.Sasao, K.Sato, K.N.Sato, F.Shinbo, H.Takahashi, S.Tanahashi, Y.Taniguchi, K.Toi and T.Tsuzuki, *Application of Intermediate Frequency Range Fast Wave to JIPP T-IIU Plasma*; Sep.1990

NIFS-49 A.Kageyama, K.Watanabe and T.Sato, *Global Simulation of the Magnetosphere with a Long Tail: The Formation and Ejection of Plasmoids*; Sep.1990

NIFS-50 S.Koide, *3-Dimensional Simulation of Dynamo Effect of Reversed Field Pinch*; Sep. 1990

NIFS-51 O.Motojima, K. Akaishi, M.Asao, K.Fujii, J.Fujita, T.Hino, Y.Hamada, H.Kaneko, S.Kitagawa, Y.Kubota, T.Kuroda, T.Mito, S.Morimoto, N.Noda, Y.Ogawa, I.Ohtake, N.Ohyabu, A.Sagara, T. Satow, K.Takahata, M.Takeo, S.Tanahashi, T.Tsuzuki, S.Yamada, J.Yamamoto, K.Yamazaki, N.Yanagi, H.Yonezu, M.Fujiwara, A.Iiyoshi and LHD Design Group, *Engineering Design Study of Superconducting Large Helical Device*; Sep. 1990

NIFS-52 T.Sato, R.Horiuchi, K. Watanabe, T. Hayashi and K.Kusano, *Self-Organizing Magnetohydrodynamic Plasma*; Sep. 1990

NIFS-53 M.Okamoto and N.Nakajima, *Bootstrap Currents in Stellarators and Tokamaks*; Sep. 1990

NIFS-54 K.Itoh and S.-I.Itoh, *Peaked-Density Profile Mode and Improved Confinement in Helical Systems*; Oct. 1990

NIFS-55 Y.Ueda, T.Enomoto and H.B.Stewart, *Chaotic Transients and Fractal Structures Governing Coupled Swing Dynamics*; Oct. 1990

NIFS-56 H.B.Stewart and Y.Ueda, *Catastrophes with Indeterminate Outcome*; Oct. 1990

NIFS-57 S.-I.Itoh, H.Maeda and Y.Miura, *Improved Modes and the Evaluation of Confinement Improvement*; Oct. 1990

NIFS-58 H.Maeda and S.-I.Itoh, *The Significance of Medium- or Small-size Devices in Fusion Research*; Oct. 1990

NIFS-59 A.Fukuyama, S.-I.Itoh, K.Itoh, K.Hamamatsu, V.S.Chan, S.C.Chiu, R.L.Miller and T.Ohkawa, *Nonresonant Current Drive by RF Helicity Injection*; Oct. 1990

NIFS-60 K.Ida, H.Yamada, H.Iguchi, S.Hidekuma, H.Sanuki, K.Yamazaki and CHS Group, *Electric Field Profile of CHS Heliotron/Torsatron Plasma with Tangential Neutral Beam Injection*; Oct. 1990

NIFS-61 T.Yabe and H.Hoshino, *Two- and Three-Dimensional Behavior of Rayleigh-Taylor and Kelvin-Helmholz Instabilities*; Oct. 1990

NIFS-62 H.B. Stewart, *Application of Fixed Point Theory to Chaotic Attractors of Forced Oscillators;* Nov. 1990

NIFS-63 K.Konn., M.Mituhashi, Yoshi H.Ichikawa,*Soliton on Thin Vortex Filament;* Dec. 1990

NIFS-64 K.Itoh, S.-I.Itoh and A.Fukuyama,*Impact of Improved Confinement on Fusion Research;* Dec. 1990

NIFS -65 A.Fukuyama, S.-I.Itoh and K. Itoh,*A Consistency Analysis on the Tokamak Reactor Plasmas;* Dec. 1990

NIFS-66 K.Itoh, H. Sanuki, S.-I. Itoh and K. Tani,*Effect of Radial Electric Field on α-Particle Loss in Tokamaks;* Dec. 1990

NIFS-67 K.Sato,and F.Miyawaki,*Effects of a Nonuniform Open Magnetic Field on the Plasma Presheath*; Jan.1991

NIFS-68 K.Itoh and S.-I.Itoh,*On Relation between Local Transport Coefficient and Global Confinement Scaling Law;* Jan. 1991

NIFS-69 T.Kato, K.Masai, T.Fujimoto,F.Koike, E.Källne, E.S.Marmar and J.E.Rice,*He-like Spectra Through Charge Exchange Processes in Tokamak Plasmas;* Jan.1991

NIFS-70 K. Ida, H. Yamada, H. Iguchi, K. Itoh and CHS Group, *Observation of Parallel Viscosity in the CHS Heliotron/Torsatron* ; Jan.1991

NIFS-71 H. Kaneko, *Spectral Analysis of the Heliotron Field with the Toroidal Harmonic Function in a Study of the Structure of Built-in Divertor* ; Jan. 1991

NIFS-72 S. -I. Itoh, H. Sanuki and K. Itoh, *Effect of Electric Field Inhomogeneities on Drift Wave Instabilities and Anomalous Transport* ; Jan. 1991

NIFS-73 Y.Nomura, Yoshi.H.Ichikawa and W.Horton,*Stabilities of Regular Motion in the Relativistic Standard Map;* Feb. 1991

NIFS-74 T.Yamagishi, *;Electrostatic Drift Mode in Toroidal Plasma with Minority Energetic Particles,* Feb. 1991

NIFS-75 T.Yamagishi, *Effect of Energetic Particle Distribution on Bounce Resonance Excitation of the Ideal Ballooning Mode,* Feb. 1991

NIFS-76 T.Hayashi, A.Takei, N.Ohybu, T.Sato, *Suppression of Magnetic Surface Breaking by Simple Extra Coils in Finite Beta Equilibrium of Helical System*; Feb. 1991

NIFS-77 N.Ohyabu, *High Temperature Divertor Plasma Operation;* Feb. 1991

NIFS-78 K.Kusano, T.Tamano and T.Sato, *Simulation Study of Toroidal Phase-Locking Mechanism in Reversed-Field Pinch Plasma;* Feb. 1991